

## **SANDIA REPORT**

SAND2004-5466  
Unlimited Release  
Printed November 2004

# **Magnetophoretic Bead Trapping in a High-Flowrate Biological Detection System**

Conrad D. James, Paul C. Galambos, Mark Derzon, Matthew Hopkins, G. Ronald Anderson, Paul Clem, Thomas Lemp, James Martin, Kamyar Rahimian, Lauren Rohwer

Prepared by  
Sandia National Laboratories  
Albuquerque, New Mexico 87185 and Livermore, California 94550

Sandia is a multiprogram laboratory operated by Sandia Corporation, a Lockheed Martin Company, for the United States Department of Energy's National Nuclear Security Administration under Contract DE-AC04-94AL85000.

Approved for public release; further dissemination unlimited.



Issued by Sandia National Laboratories, operated for the United States Department of Energy by Sandia Corporation.

**NOTICE:** This report was prepared as an account of work sponsored by an agency of the United States Government. Neither the United States Government, nor any agency thereof, nor any of their employees, nor any of their contractors, subcontractors, or their employees, make any warranty, express or implied, or assume any legal liability or responsibility for the accuracy, completeness, or usefulness of any information, apparatus, product, or process disclosed, or represent that its use would not infringe privately owned rights. Reference herein to any specific commercial product, process, or service by trade name, trademark, manufacturer, or otherwise, does not necessarily constitute or imply its endorsement, recommendation, or favoring by the United States Government, any agency thereof, or any of their contractors or subcontractors. The views and opinions expressed herein do not necessarily state or reflect those of the United States Government, any agency thereof, or any of their contractors.

Printed in the United States of America. This report has been reproduced directly from the best available copy.

Available to DOE and DOE contractors from  
U.S. Department of Energy  
Office of Scientific and Technical Information  
P.O. Box 62  
Oak Ridge, TN 37831

Telephone: (865)576-8401  
Facsimile: (865)576-5728  
E-Mail: [reports@adonis.osti.gov](mailto:reports@adonis.osti.gov)  
Online ordering: <http://www.osti.gov/bridge>

Available to the public from  
U.S. Department of Commerce  
National Technical Information Service  
5285 Port Royal Rd  
Springfield, VA 22161

Telephone: (800)553-6847  
Facsimile: (703)605-6900  
E-Mail: [orders@ntis.fedworld.gov](mailto:orders@ntis.fedworld.gov)  
Online order: <http://www.ntis.gov/help/ordermethods.asp?loc=7-4-0#online>



SAND2004-5466  
Unlimited Release  
Printed March 2005

## **Magnetophoretic Bead Trapping in a High-Flowrate Biological Detection System**

Conrad D. James, Paul C. Galambos  
MEMS Device Technologies

Mark Derzon  
MESA Microfabrication

Matthew Hopkins  
Multiphase Transport Processes

G. Ronald Anderson  
Micro-product Engineering

Paul Clem  
Microsystems Materials & Mechanical Behavior

Thomas Lemp  
Photonic Microsystems Technology

James Martin  
Nanostructure & Semiconductor Physics

Kamyar Rahimian  
Organic Materials Aging & Reliability

Lauren Rohwer  
Back-end-of-the-line Advanced Packaging

Sandia National Laboratories  
P.O. Box 5800  
Albuquerque, New Mexico 87185-1080

## Abstract

This report contains the summary of the “Magnetophoretic Bead Trapping in a High-Flowrate Biological Detection System” LDRD project 74795. The objective of this project is to develop a novel biodetection system for high-throughput sample analysis. The chief application of this system is in detection of very low concentrations of target molecules from a complex liquid solution containing many different constituents – some of which may interfere with identification of the target molecule. The system is also designed to handle air sampling by using an aerosol system (for instance a WESP – Wet Electro-Static Precipitator, or an impact spray system) to get air sample constituents into the liquid volume. The system described herein automatically takes the raw liquid sample, whether air converted or initially liquid matrix, and mixes in magnetic detector beads that capture the targets of interest and then performs the sample cleanup function, allowing increased sensitivity and eliminating most false positives and false negatives at a downstream detector.

The surfaces of the beads can be functionalized in a variety of ways in order to maximize the number of targets to be captured and concentrated. Bacteria and viruses are captured using antibodies to surface proteins on bacterial cell walls or viral particle coats. In combination with a cell lysis or PCR (Polymerase Chain Reaction), the beads can be used as a DNA or RNA probe to capture nucleic acid patterns of interest. The sample cleanup capability of this system would allow different raw biological samples, such as blood or saliva to be analyzed for the presence of different infectious agents (e.g. smallpox or SARS). For future studies, we envision functionalizing bead surfaces to bind to chemical weapons agents, radio-isotopes, and explosives.

The two main objectives of this project were to explore methods for enhancing the mixing of the capture microspheres in the sample, and to develop a novel high-throughput magnetic microsphere trap. We have developed a novel technique using the magnetic capture microspheres as “stirrer bars” in a fluid sample to enhance target binding to the microsphere surfaces. We have also made progress in developing a polymer-MEMS electromagnet for trapping magnetic spheres in a high-flowrate fluid format.

## **Contents**

Contents	5
Figures	6
Nomenclature	7
<b>Introduction</b>	<b>8</b>
<b>1.0 System Description</b>	<b>8</b>
1.1 Unique Features.....	9
<b>2.0 Sample Mixing</b>	<b>10</b>
<b>3.0 Magnetic Trap</b>	<b>11</b>
3.1 Magnetophoresis theory.....	11
3.2 Magnetophoretic Trapping Experiments.....	13
3.3 Second prototype Trap Fabrication .....	15
<b>Conclusion</b>	<b>17</b>
<b>Acknowledgements</b>	<b>19</b>
<b>References</b>	<b>20</b>
<b>Distribution:</b>	<b>21</b>

## Figures

- Figure 1. Conceptual layout for a multiple trace pathogen collection system. 9
- Figure 2. Schematic of the tri-axial magnetic Helmholtz coil used to characterize the effect of mixing on detection rate (left). Mixing of magnetic particles using the triaxial magnetic field system (right). 10
- Figure 3. Comparison of magnetic mixing with diffusion and manual pipette mixing for bovine serum and buffer at constant conditions. 11
- Figure 4. Simulations of  $\nabla B^2(x, z)$  generated from different EM wire configurations (left). Lineplot comparisons of  $\nabla B^2(x, z_o = 10\mu m)$  at the dashed red lines in the left panel (right). 12
- Figure 5. Flowing beads becoming trapped along the EM wire in a fluidic channel (top). Particle velocity as a function of radial distance from the wire (bottom). 13
- Figure 6. Bead velocity (dashed lines) and time to capture (solid lines) as a function of the distance from the EM wire and the tapping current. 14
- Figure 7. Bead velocity induced by the magnetic field as a function of  $I^2$  and as a function of distance from the EM wire (colors). 15
- Figure 8. a) Top view of the trap depicting EM wires (black) written on patterned polymer. b) Side view of EM wires inside channels. c) View of the rolled microfluidic device. 16
- Figure 9: Printed silver lines on a Kapton Film(top). Close-up of needle printed silver lines (bottom). 17
- Figure 10. Characteristics of robocasted silver wires. 18

## **Nomenclature**

DI	deionized
DNA	deoxyribonucleic acid
EM	electromagnet
LDRD	Laboratory Directed Research and Development
PCR	Polymerase Chain Reaction
RNA	ribonucleic acid
SARS	severe acute respiratory syndrome
SNL	Sandia National Laboratories
WESP	Wet electrostatic precipitator

## Introduction

This SAND report contains a description of the work performed and results of Late Start LDRD “Magnetophoretic Bead Trapping in a High-Flowrate Biological Detection System” LDRD project 74795. The objective of this LDRD was to develop techniques and microsystem configurations for a meso-scale (~mm) fluidic handling system. The system utilizes magnetic beads with built-in identification tags and surface functionalizations to capture targets (bioagents, chemical warfare agents, explosives, and radiological species) and extract these targets from fluid samples for rapid detection. Both bead mixing and sample cleanup (bead extraction and fluid exchange) will be accomplished in the same system using magnetophoresis implemented through an electromagnet.

Significant results include the demonstration of efficient fluid mixing using a three-dimensional magnetic field system. Magnetophoretic trapping of microspheres flowing in polymeric fluid channels was also demonstrated under various buffer conditions. Both the mixing and the trapping exhibit excellent characteristics nearly independent of solution conductivity and pH. Surrogate solutions for bovine blood serum, urine and milk were successfully tested, as well as strawberry juice and water solutions.

### 1.0 System Description

The chief application of this system is to create components for a system capable of detecting very low concentrations of target molecules from a complex liquid solution containing many different constituents – some of which may interfere with identification of the target molecule. A basic system and all the necessary components is shown in Fig. 1. The system contains an air sampling unit (for instance a WESP – Wet Electro-Static Precipitator, or an impact spray system) to get air sample constituents into a liquid volume. The high volume air flow and particulate collection occurs in the WESP, mixing and hybridization of molecular recognition tags with analytes of interest occurs in (2), sample cleanup and bead concentration in (3), and positive determination and identification occur in the detector sub-system (4). The system described herein automatically takes the raw liquid sample, whether air converted or initially liquid matrix, and mixes in magnetic detector beads that capture the targets of interest and then performs the sample cleanup function, allowing increased sensitivity and reducing false positives and false negatives at a downstream detector. This LDRD was limited to obtaining proof-of-principal data regarding the ability to perform the functions of the mixing and trapping components.



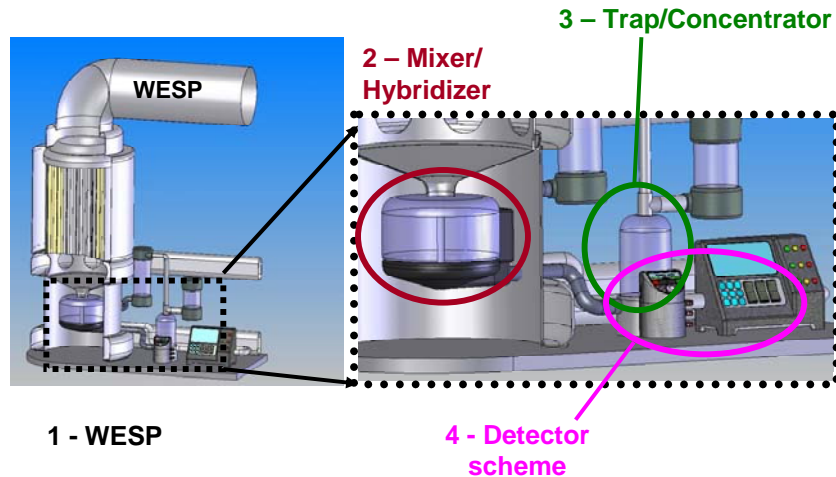


**Figure 1. Conceptual layout for a multiple trace pathogen collection system.**

The surfaces of the beads can be functionalized in a variety of ways, and many research groups and companies specialize in surface functionalization. Only the mixing and extraction of the functionalized magnetic beads are reported here. Different applications can be addressed by using different surface functionalizations. Functionalizing bead surfaces with antibodies to different proteins enables the beads to capture various biological toxins, viruses, and/or bacteria. Bacteria and viruses are captured using antibodies to surface proteins on bacterial cell walls or viral particle coats. In combination with a cell lysis or PCR (Polymerase Chain Reaction) unit, the beads can be used as a DNA or RNA probe to capture nucleic acid patterns of interest. The sample cleanup capability of this system would allow different biological samples, such as blood or saliva, to be analyzed for the presence of different infectious agents (e.g. smallpox or SARS). Similarly, by functionalizing bead surfaces to bind to chemical weapons agents and explosive vapors, a detection system can be developed that could be used to detect traces of chemical agents and explosives in various settings. Finally by functionalizing bead surfaces to bind to different radio-isotopes, a type of a radiation getter can be developed for identification and concentration of radiation at very low levels as might be in the air in the vicinity of a dirty bomb.

### 1.1 Unique Features

The unique features of the system are robust and multiple raw sampling handling (reduced processing steps) as well as enabling the detection of lower concentrations than is presently possible. Additional unique features are enhanced mixing speed (reduced total assay time), cost, scalability in flow volume, general WMD capability (rather than exclusive biological, chemical or nuclear detection), and avoiding the need for sample preparation. Basically, the system should work for any substance which is identifiable with a molecular

recognition tag whose chemistry is compatible with the bead and detector chemistry/photronics.

## 2.0 Sample Mixing

Our mixing system uses a triaxial magnetic field described in Martin et al. [1]. This technique uses three nested Helmholtz coils [Fig. 2, left] to generate oscillatory motion in magnetic particles suspended in fluids. By manipulating the 3 fields, magnetic particles that are initially pulled to one wall can be almost instantaneously mixed into the sample volume [Fig. 2, right]. The time between images (1) and (2) is < 1 second. A fraction of a second after image (2) was captured, the magnetic particles are uniformly distributed throughout the test tube volume (1 ml test tube) and the image is completely black. Horizontal and vertical lines of particles (3) can also be generated by magnetic field manipulation.

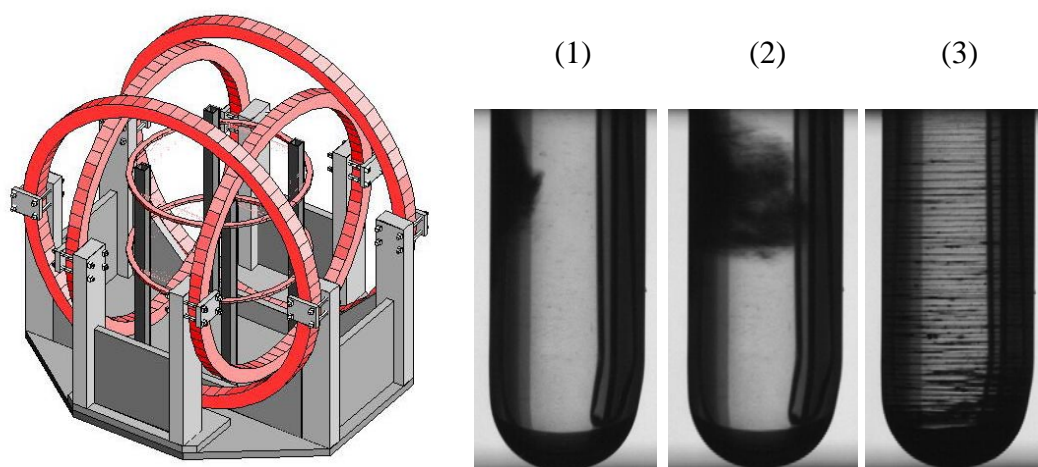


**Figure 2. Schematic of the tri-axial magnetic Helmholtz coil used to characterize the effect of mixing on detection rate (left). Mixing of magnetic particles using the triaxial magnetic field system (right).**

We performed a series of experiments with streptavidin-coated beads in biotin-laced buffer solution. Streptavidin coated immunomagnetic beads are magnetite nanoparticles coated with a thin layer of polystyrene, immunoactivated with cross-linkers, and then coated with many thousands of streptavidin molecules each capable of binding four biotin molecules.

We expect the fraction of targets bound to grow exponentially until saturation, with the exponential growth rate proportional to (number of beads) x (characteristic mixing speed) x (square of bead radius). The exponential form of the fraction binding is exhibited in Fig. 3. The magnetic mixing outperforms diffusion, while not attaining the mixing efficiency of manual pipette mixing. However, we have not yet performed parameterized scaling and optimization of

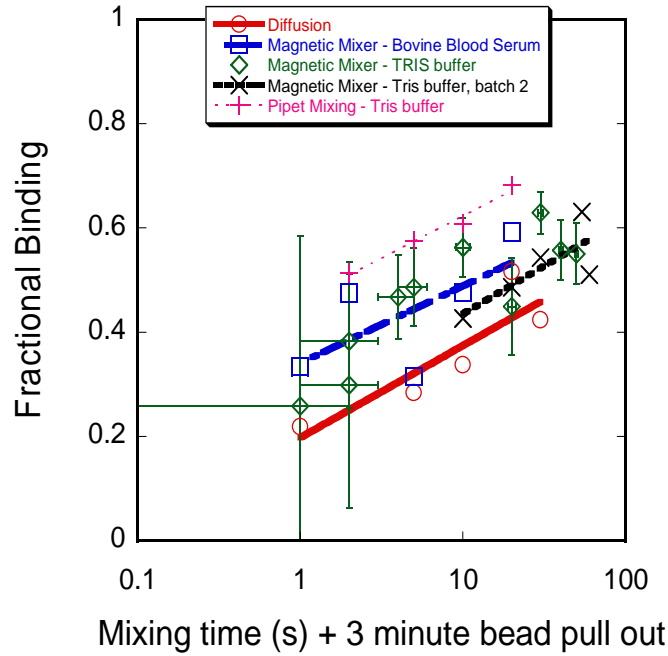


**Figure 3. Comparison of magnetic mixing with diffusion and manual pipette mixing for bovine serum and buffer at constant conditions.**

mixing characteristics by manipulating frequency, axial field strength, and excitation waveform.

### 3.0 Magnetic Trap

The magnetic beads will be trapped using an electromagnet that can be turned on or off to facilitate controlled capture of beads and thus concentration of targets. We are exploring the use of polymer substrates and novel metal deposition techniques to develop a sheet-goods producible trap at significantly lower cost and high fabrication throughput.

#### 3.1 Magnetophoresis theory

The trap consists of a set of flow channels with embedded wires that act as electromagnets (EM). The passage of a current  $I$  through the wire will generate a magnetic flux density,  $B$  [2]:

$$B = \frac{\mu_0 I}{2\pi r} \quad \text{Eq. 1}$$

where  $\mu_0$  is the permeability of free space, and  $r$  is the radial distance from the wire. If the generated magnetic flux density is non-uniform ( $\nabla B^2 \neq 0$ ), a

magnetophoretic force is generated on a particle with radius  $r_p$ , and permeability  $\mu_p$  [3]:

$$F_{mag} = 2\pi \frac{\mu_p - \mu_f}{\mu_p + 2\mu_f} r_p^3 \frac{\nabla B^2}{\mu_f} \quad \text{Eq. 2}$$

where  $\mu_f$  is the permeability of the fluid. When a magnetic particle is pulled toward the electromagnet wire under the trapping force, an opposing drag force is also generated on the particle,  $F_{drag} = 6\pi\eta r_p v_p$ , where  $\eta$  is the fluid viscosity, and  $v_p$  is the particle velocity with respect to the fluid velocity. Due to the fact that the drag force scales linearly with the particle radius, while the trapping force scales to the third power of the particle radius, we chose larger particles ( $\sim 10 \mu\text{m}$ ) to enhance the trapping effect. Eq. 2 also predicts that the trapping force

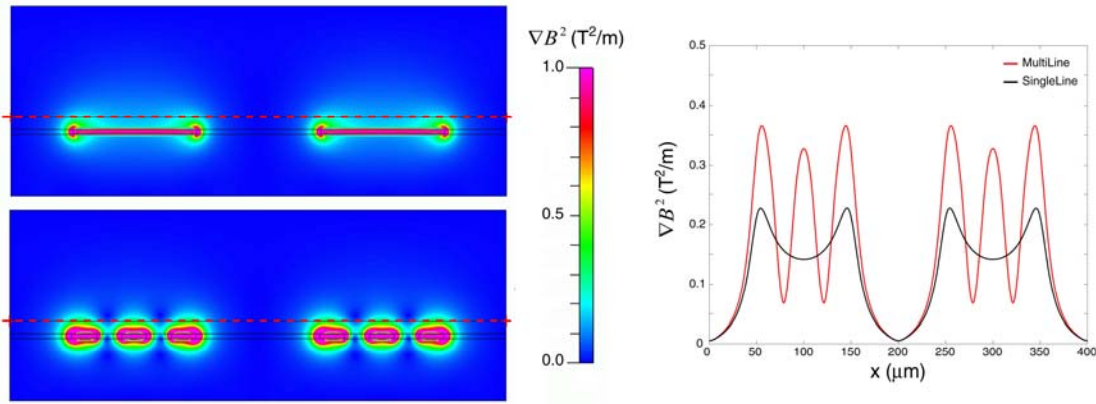


**Figure 4. Simulations of  $\nabla B^2(x, z)$  generated from different EM wire configurations (left). Lineplot comparisons of  $\nabla B^2(x, z_o = 10 \mu\text{m})$  at the dashed red lines in the left panel (right).**

scales as the square of  $B$  (which is proportional to the current  $I$  in the wire), and inversely proportional to the length-scale  $x$  of the electromagnet wire ( $\nabla B^2 = \partial B^2 / \partial x$ ). Simulations of  $\nabla B^2$  for different currents and wire length-scales shows that sufficient trapping force can be generated with moderate currents (500 mA) and moderate wire dimensions (10-100  $\mu\text{m}$  width, 4  $\mu\text{m}$  thickness). Fig. 4 shows a simulation of two 100  $\mu\text{m}$  wide, 4  $\mu\text{m}$  thick wires each carrying 333 mA (top, left). The bottom, left panel shows two sets of wires, each with three 20  $\mu\text{m}$  wide lines, spaced by 20  $\mu\text{m}$ . Each line carries 111 mA, producing a total of 666 mA for the total set of wires. The total amount of current being carried in each case is the same (666 mA), but the different length scales of the wire features lead to differences in the generated  $\nabla B^2$ . The right panel of Fig. 4 shows line

plots of both cases, indicating that the wire configuration has a significant effect on the distribution of the trapping force ( $\nabla B^2$ ).

### 3.2 Magnetophoretic Trapping Experiments

Initial experiments were performed with machined PMMA substrates with 1 mm wide and 0.5 mm height single channels. Wires of various dimension were placed and glued onto the channel floor to serve as electromagnets. Parylene deposition was used to insulate EM wires in several experiments. Contacts to the

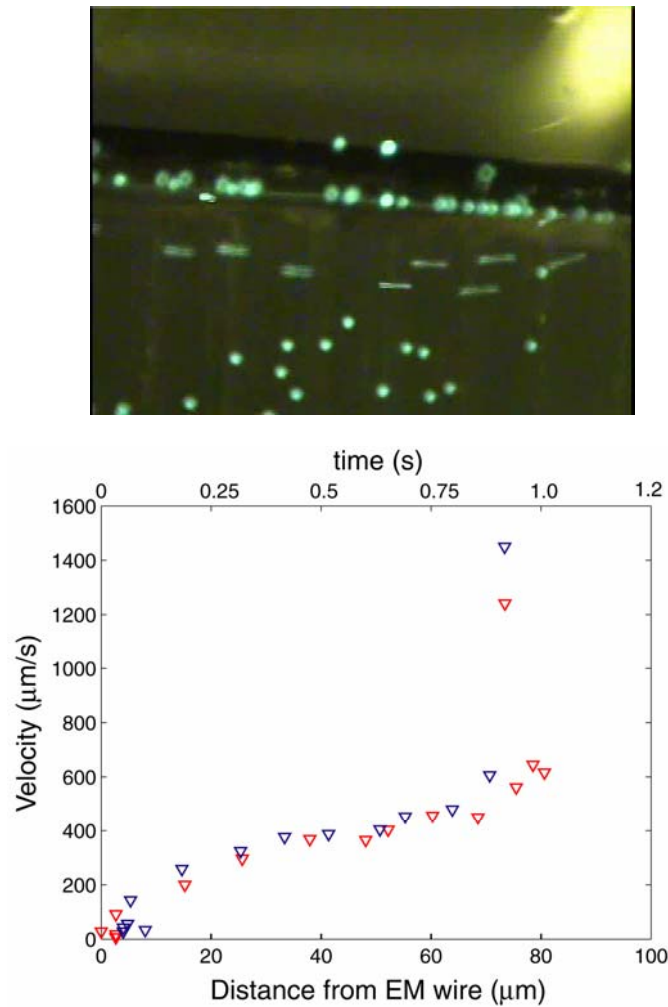


**Figure 5. Flowing beads becoming trapped along the EM wire in a fluidic channel (top). Particle velocity as a function of radial distance from the wire (bottom).**

electromagnet wires were made with copper tape and silver epoxy, and channels were closed with cover glass, double-sided tape, and epoxy for sealing leaks. Capillaries were glued into place for inlets and outlets.

In different versions of the system, these EM wires can be replaced by permanent magnets, but the base configuration uses EMs. The set of channels make up a 3D array allowing parallel flow of a significant volume of liquid through the device while still allowing individual channels to be small (on the order of 100 to 500 microns deep) so that large magnetic field gradients can be applied to the particles in the channels. The magnetic particles generally consist of magnetite embedded in polystyrene or some other plastic coating that is functionalized as described above. Fig. 5 shows an 80  $\mu\text{m}$  diameter wire carrying 1 A of current. The velocity plot tracks two particles (red and blue) initially traveling at 500  $\mu\text{m/s}$  at a radial distance of  $\sim 70 \mu\text{m}$  from the wire. At this initial distance, both particles were trapped to the wire in less than 1 second, which means they were trapped after traveling  $\sim 500 \mu\text{m}$  parallel to the wire. These experiments have allowed us to design the device parameters to optimize bead trapping efficiency in terms of both speed of capture, and distance traveled along the channel before capture. Fig. 6 shows the magnetophoresis-induced velocity and time to capture of

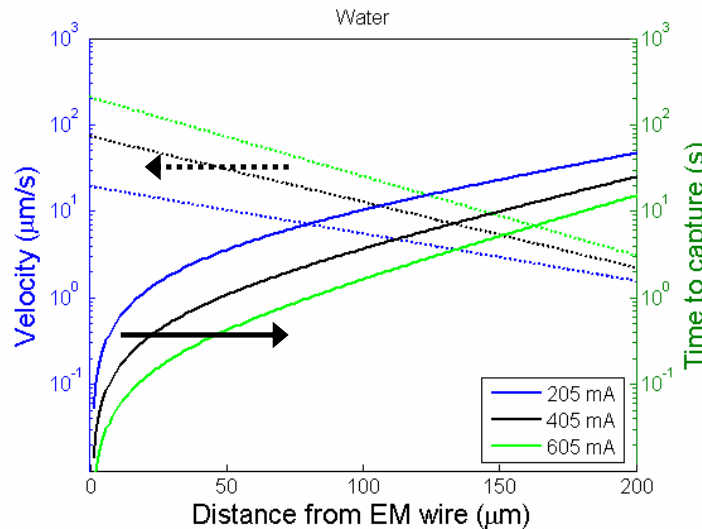


**Figure 6. Bead velocity (dashed lines) and time to capture (solid lines) as a function of the distance from the EM wire and the tapping current.**

8.5  $\mu\text{m}$  diameter magnetic beads suspended in DI water using a 25  $\mu\text{m}$  diameter EM wire. As the current through the wire increases, the velocity increases and the time to trap decreases. An increase in velocity leads to a reduction in the amount of time required to capture the bead to the trap. These trapping experiments have also been performed in several fluids with different conductivities and pH, including blood, urine, and bile stimulant buffers. The magnetophoretic trapping works similarly under all conditions. Fig. 7 indicates that the trap-induced velocity is as expected - roughly linear with the squared current through the EM wire.

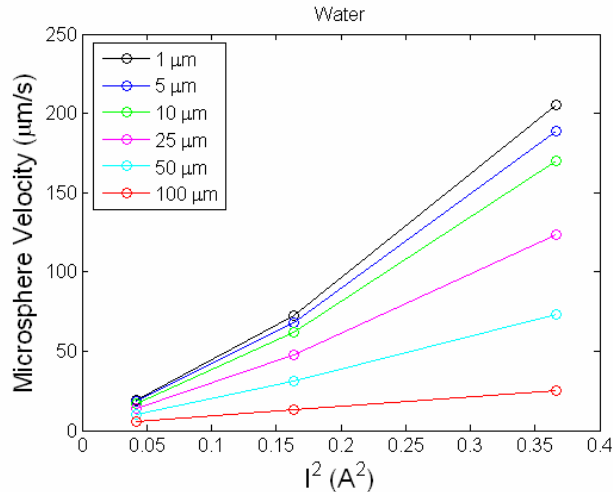


**Figure 7. Bead velocity induced by the magnetic field as a function of  $I^2$  and as a function of distance from the EM wire (colors).**

### 3.3 Second prototype Trap Fabrication

The first trap prototype discussed previously can be adapted to a more mass producible format such as that shown in Fig. 8. This fabrication technique utilizes hot embossing to deform plastic materials into channels that can then be rolled up to form an array of parallel flow channels. Electrodes are patterned onto the plastic sheets allowing parallel electromagnetic traps to be localized within each channel. These traps can all be accessed simultaneously with a single voltage source. The corrugations in the sheet provide the channel dimensions, and using our simulations and experimental data, we have determined good ranges for the channel dimensions that optimize the trapping efficiency.

Many different plastic materials, including but not limited to PMMA and Kapton, can be used to fabricate the array of channels. The key property of the material is that the plastic deformation temperature required for the hot embossing process not be too low (150-180 C typical) so that the processing required to cure the wire traces does not deform the sheet of plastic. Typically embossing is done before wire trace deposition. Sheets of acrylic (PMMA) and Kapton have been hot embossed to depths of between 10's of microns to a few mm. Typically embossing molds are made from steel and can be used 100's of times allowing mass production of channels.

An alternative method of making the plastic channel array required for the array of traps is to mold plastic sheets. Injection molding could be one method for mass production but there is nothing limiting us to that technique.

A 3<sup>rd</sup> promising method of fabricating the channels involves the use of PDMS (polydimethylsiloxane) and 'soft lithography' processes [4]. Such a



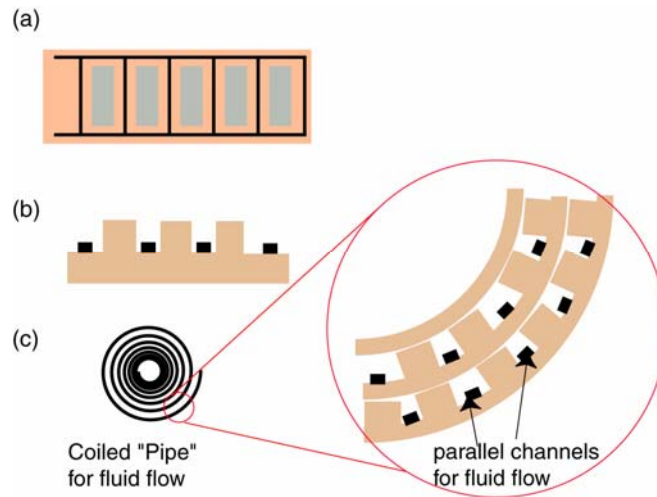


**Figure 8. a) Top view of the trap depicting EM wires (black) written on patterned polymer. b) Side view of EM wires inside channels. c) View of the rolled microfluidic device.**

soft lithography process can be adapted to our array of channels by patterning PDMS on top of a hard plastic substrate and then closing the channels with a cover lid of plastic. Glass could also be used in the rectangular stacked configuration as opposed to the rolled configuration. In either configuration, the PDMS becomes the sidewall of the trapping or mixing flow channel.

### 3.31 Wire Printing

The metal electrodes will be written using a technology covered in the technical advance number SD-7815/S-104.550. The concept uses a thermal reduction-oxidation process between a metallic salt as the oxidizing agent, such as silver nitrate, and a polymeric material as the reducing agent, such as polyvinyl alcohol. A solution of the metal salt and the polymer is used to deposit lines inside the channels of the polymeric substrate, after which thermal processing (for  $\text{AgNO}_3/\text{PVA}$  heating above 150C for several minutes) of this mixture induces the redox chemistry and leaves behind a metallic substance (silver for  $\text{AgNO}_3/\text{PVA}$ ). The writing process can be accomplished using several techniques, including but not limited to: ink-jet printing (Fig. 9), robocasting [5] (Fig. 10), and micropen instrumentation. The thickness and width of electrodes can be controlled by inducing variations in the writing technique.





**Figure 9: Printed silver lines on a Kapton Film(top). Close-up of needle printed silver lines (bottom).**

Figure 9 shows silver lines that were printed on a Kapton film. The thinnest line-width on this sample was 300  $\mu\text{m}$ , and this was accomplished using a 100  $\mu\text{m}$  diameter nozzle. AFM measurements showed the lines are 2.2  $\mu\text{m}$  thick, with a transition length of 30  $\mu\text{m}$  (distance from the edge of the line to the point on the line that is at full thickness). The line-width and thickness can be controlled somewhat by varying the viscosity of the silver nitrate solution.

In Fig. 10, we summarize some of the results from robocasting, where channels down to 100  $\mu\text{m}$  were made. One of the conclusions is that using higher curing temperatures leads to higher conductivities of the silver films.

### **Conclusion**

This LDRD has produced significant advancements towards development of a novel high-throughput biodetection system. The primary areas of investigation were: capture of targets from a real-world sample, concentration of captured targets using a novel microfluidic device, and developing magnetic microspheres to serve as capture-and-carry chaperones for concentrating/separating targets and in back-end detection. The first task investigated using the magnetic microsphere chaperones as magnetic stirrers. We conducted mixing tests using different methods of mixing, and determined that the magnetic mixing of the sample increased hybridization speed and efficiency. The second task was to develop methods for producing a prototype

## Silver salt decomposition for 150°C SLA integration

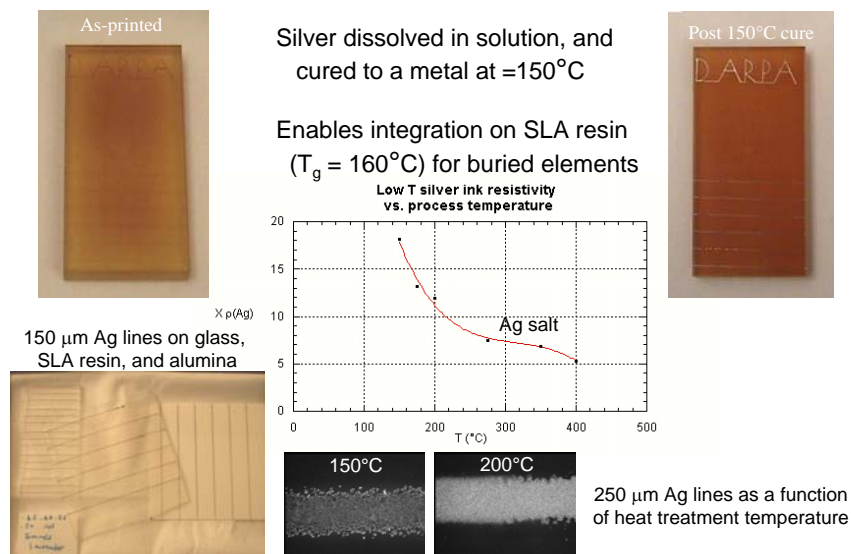


**Figure 10. Characteristics of robocasted silver wires.**

polymer-based microfluidic device for trapping magnetic particles. Early experiments demonstrated significant trapping forces being generated with currents on the order of several hundred milliamps. We have also examined the trapping efficiency as a function of distance from the electromagnet, fluid suspension properties, and magnetic field gradient. The second stage prototype will be fabricated using embossing of polymers and printing of silver nitrate onto substrates. This will enable the rapid production of roll-to-roll fabricated polymer microfluidics devices.

Smaller components of the projects ultimate goal have also been addressed: discussing options for producing a wet-electrostatic precipitator with modified design requirements to meet portable specifications, performing calculations to determine appropriate mixing and hybridization conditions, and investigating possibilities for an orthogonal assay for back-end detection. In addition, we began the initial development of a magnetic microsphere, with target-specific surface functionalizations, and internal “bar-codes” in the form of quantum dot assemblies.

## **Acknowledgements**

This LDRD has been made successful by the contributions of many individuals, both internal and external to SNL. We had very useful discussions with Doug Chinn, Stan Kravitz, Jeb Flemming, and some of the team members throughout the course of this project to get ideas on how to proceed with meeting our objectives. Jordan Knepper served as an undergraduate student intern in 01769 and 017382 provided much of the leg work on the magnetic mixing experiments, and the ink-jet printing on films work. Paul Reynolds of TEAM Specialty Products conducted work in developing an embossing tool used for fabricating channels in polymer substrates. Jaime Reif, a technologist in 01769, and Thayne Edwards, a summer intern in 01769, assisted on the magnetic trapping experiments. Lab staffers Amanda Lopez and Ken Pohl were also crucial in conducting the experimental work in the lab. Sandia is a multiprogram laboratory operated by Sandia Corporation, a Lockheed Martin Company, for the United States Department of Energy under contract DE-ACO4-94-AL85000.

## References

1. Martin, J.E., Anderson, R.A., Williamson, R.L., "Generating strange magnetic and dielectric interactions: Classical molecules and particle foams," J. Chem. Phys., 2003, Vol. 118, pp. 1557-1570.
2. Griffiths, D. J., "Introduction to Electrodynamics", 1989, 2<sup>nd</sup> edition, Prentice-Hall, Inc., Englewood Cliffs, New Jersey.
3. Jones, T.B., "Electromechanics of particles," pg. 221, 1995, Cambridge University Press, New York City, NY.
4. Deng, T., Whitesides, G.M., Radhakrishnan, M., Zabow, G., Prentiss, M., "Manipulation of magnetic microbeads in suspension using micromagnetic systems fabricated with soft lithography", Applied Physics Letters, 2001, Vol. 78, no. 12, pp 1775-1777.
5. J. Cesarano III and P. Calvert, "Freeforming Objects with Low-Binder Slurry" US Patent No. 6,027,326.

**Distribution:**

1	MS1080	Conrad James	01769
1	MS1080	Paul Galambos	01769
1	MS1425	Mark Derzon	01740
1	MS0834	Matthew Hopkins	09114
1	MS0344	Thomas Lemp	01743
1	MS0888	Kamyar Rahimian	01811
1	MS1411	Paul Clem	01851
1	MS0892	Lauren Rohwer	01745
1	MS1073	G. Ronald Anderson	017382
1	MS1080	David Sandison	01769
1	MS1073	David Peterson	017381
1	MS1421	James Martin	01112
1	MS0603	Stanley Kravitz	01763
1	MS1425	Jeb Flemming	01744
1	MS0123	Donna Chavez	01011
1	MS9018	Central Technical File	8945-1
2	MS0899	Technical Library	9616